

# Ultraprecise optical frequency standards based on ultracold atoms: state of the art and prospects

A V Taichenachev, V I Yudin, S N Bagayev

DOI: 10.3367/UFNe.0186.201602j.0193

## Contents

1. Introduction	184
2. Method of magnetically induced spectroscopy of strongly forbidden optical transitions	186
3. Generalized Ramsey method in ultra-high resolution spectroscopy of ultracold atoms and ions	189
4. Synthetic frequency method	191
5. Conclusions	193
References	194

**Abstract.** We briefly describe the current state of research in the rapidly developing field of optical frequency standards using optically and electromagnetically trapped ultracold atoms and ions. The primary emphasis is on the new spectroscopic techniques developed at the Institute of Laser Physics, SB RAS, to improve the stability and precision of current optical frequency standards.

**Keywords:** quantum frequency standards, laser cooling, Ramsey method, magic wavelength, Paul trap, optical lattice, laser

## 1. Introduction

It is well known that one of the main achievements of microwave quantum electronics is the development of quantum frequency standards, on which the atomic time scale TAI (French: Temps Atomique International) was based. Since 1967, these standards have been used to define units of time and frequency in the International System of units. The development of coherent visible light sources stimulated research on laser frequency stabilization by linking it to the center of a quantum transition in atoms, ions, and molecules. In other words, the investigation of quantum standards for optical frequencies started almost immediately after the invention of lasers.

The advantages of replacing the microwave band with the optical one are obvious: the operating frequency and quality

factor of the reference resonance increase along with the relative stability of the standard [see Eqn (1) below].

It was already known earlier that after scaling the optical frequency down to the microwave region, the relative stability is maintained in principle. But this important advantage of optical frequency standards was almost completely concealed in the first steps of research, due to physical effects associated with the translational motion of elementary radiators (mainly the Doppler broadening of the spectral line) and technical problems of scaling the frequency by a factor of  $10^5$ . Nevertheless, by using the methods of nonlinear laser spectroscopy with ultra-high resolution [1], it was possible to significantly increase the stability of optical standards (from  $10^{-8}$  to  $10^{-14}$ ) and create the first systems for optical frequency scaling. The achievements of the first stages of developing optical frequency standards are quite well described in reviews [2, 3] and monographs [1, 4].

The last decade was marked by great achievements in ultra-high resolution spectroscopy and fundamental laser metrology. The preparation of this article was mainly motivated by the impressive recent success in improving the stability and accuracy of quantum frequency standards in the optical region. This success is connected with the development of methods for laser cooling of ions and atoms to ultra-low temperatures (of the order of 1  $\mu$ K and lower) and also for precise control over their translational and internal degrees of freedom.

Almost immediately after the invention of lasers, it was understood that laser radiation has a virtually unlimited potential to control not only internal but also translational degrees of freedom of atoms. The 1970s and 1980s are known for the useful interplay among pioneering ideas, fundamental experiments, and advanced theories. At that time, experiments on the mechanical action of laser radiation on atoms and ions were being carried out both in Russia (USSR) and abroad. In a large number of key cases, there is no doubt about the superiority of Russian scientists. For example, the idea of increasing the resolution of laser spectroscopy by localizing the atoms in optical lattices was first presented by Letokhov [5] in 1968, pioneering experiments on laser cooling of a neutral atom beam were

A V Taichenachev, V I Yudin, S N Bagayev Institute of Laser Physics, Siberian Branch, Russian Academy of Sciences, prosp. Akademika Lavrent'eva 13/3, 630090 Novosibirsk, Russian Federation; Novosibirsk State University, ul. Pirogova 2, 630090 Novosibirsk, Russian Federation  
E-mail: taichenachev@laser.nsc.ru, viyudin@mail.ru, bagayev@laser.nsc.ru

Received 9 December 2015

Uspekhi Fizicheskikh Nauk 186 (2) 193–205 (2016)

DOI: 10.3367/UFNr.0186.201602j.0193

Translated by A L Chekhov; edited by A M Semikhatov

performed at the Institute of Spectroscopy, RAS, by Balykin, Letokhov, and coauthors [6, 7], and the idea of atomic interferometry belongs to Dubetsky, Chebotayev, Kazantsev, and Yakovlev [8]. The main achievements of the first stage (until the end of 1986) of the research on laser cooling and spatial localization of atoms are described in detail in reviews [9–11] and monographs [12, 13], which also contain a comprehensive bibliography of original works.

However, due to a number of objective and subjective reasons, research activity on this topic decreased in Russia at the end of the 1980s and especially in the 1990s. As a result, the main revolutionary achievements of the second stage (after 1986) are attributed to foreign scientists. The main achievements are as follows: experimental realization of the magneto-optical trap (the main source of ultracold neutral atoms) by S Chu [14], the discovery of laser cooling overcoming the Doppler limit—a breakthrough from temperatures of the order of  $10^{-3}$  K down to lower than  $10^{-6}$  by W Phillips and coauthors [15], the development of the theory of laser cooling lower than the Doppler limit [16] and the recoil limit [17] by C Cohen-Tannoudji and coauthors, and the observation of the Bose–Einstein condensation of alkali metal neutral atoms by three different groups in 1995 [18–20]. These and other significant achievements in the field of ultracold atoms have been mentioned in many review articles (see, e.g., articles published in *Physics–Uspekhi* [21–23]) and monograph [32].

We recall the main definitions and notions of quantum metrology that are used in describing frequency-standard characteristics. For any quantum frequency standard, the frequency of the macroscopic oscillator (which is a microwave oscillator for the microwave band and a laser for the optical band) is linked to the quantum transition between two levels using a feedback system. As a result, the oscillator frequency becomes almost independent of varying macroscopic conditions, such as temperature and pressure. However, even this stabilized frequency over time experiences weak fluctuations around some mean value. The main metrological characteristics of the frequency standard are its stability and accuracy.

Frequency stability is a state in which the oscillator frequency remains constant during its continuous operation, and instability is inversely proportional to stability. Stability depends not only on the width of the spectral line but also on the resonance intensity (contrast) and noise level. To describe the relative instability  $\delta\omega/\omega$  numerically, the Allan variance [33] over some observation (averaging) time  $\tau$  is used. In the ideal case of white noise caused by the quantum nature of the detection process, the relative instability can be estimated as [34]

$$\sigma_y(\tau) \approx \frac{1}{\pi} \frac{1}{Q} \frac{1}{s/n} \sqrt{\frac{\tau_c}{\tau}}, \quad (1)$$

where  $Q$  is the quality factor of the reference resonance (the ratio between the FWHM and the resonance frequency),  $s/n$  is the signal-to-noise ratio, proportional to  $\sqrt{N}$  ( $N$  is the number of resonant atoms), and  $\tau_c$  is the duration of one measurement cycle.

Frequency standard accuracy is a state in which the average oscillator frequency coincides with the frequency of the unperturbed quantum transition (under ideal conditions). The frequency standard accuracy is connected with the uncertainty of systematic shifts of the mean oscillator

frequency relative to the frequency of an unperturbed quantum transition. There are many technical and physical reasons for these shifts to appear. For modern optical standards, the most fundamental reasons are field shifts of various natures. We note that in order to achieve high accuracy, we need to perform a thorough theoretical and experimental analysis of systematic shifts, which is almost impossible without a high stability of the standard.

Referring to modern quantum frequency standards, we can distinguish two main research fields: optical frequency standards based on ultracold single ions in radio frequency traps (like the Paul trap [35]) [36–43] and those based on ensembles of ultracold neutral atoms (with the number of atoms greater than  $10^4$ – $10^5$ ), trapped in an optical lattice at the magic wavelength (so-called optical lattice clocks) [44–46]. In both cases, elementary oscillators (single ions or atoms) become spatially localized at scales that are much shorter than the probe laser wavelength.

One of the main goals of this research is to create primary optical frequency standards with a relative frequency uncertainty of the order of  $10^{-17}$ – $10^{-18}$ . In the case of ion standards, these investigations have been conducted for more than 30 years. The best results are obtained for the standards based on the aluminum ion [47], with a relative frequency uncertainty of  $8.6 \times 10^{-18}$ , the strontium ion [48, 49], with  $1.2 \times 10^{-17}$ , and the ytterbium ion [50],  $3 \times 10^{-18}$ . Active and productive research on lattice clocks began much later, when a number of laboratories simultaneously succeeded in obtaining ultranarrow resonances at a strongly forbidden optical transition  $^1S_0 \leftrightarrow ^3P_0$  in atoms of strontium [51–53] and ytterbium [54] in 2005–2006. However, after a short period of time, the researchers achieved quite significant results [55, 56] and reached the values of relative frequency instability comparable with the best ion standards or even overcoming them. The most promising lattice clocks are the ones based on strontium and ytterbium [57–62], which have increased their stability and accuracy by an order of magnitude in the last four years: from  $1 \times 10^{-17}$  to  $2 \times 10^{-18}$ .

We note that the metrological characteristics of single-ion or lattice clocks are now significantly better than those of the first atomic standards based on the cesium fountain. This means that in the nearest future, units of time and frequency can be redefined using optical frequency standards [63]. We recall that in the International System of units, one second equals 9,192,631,770.0 periods of radiation corresponding to the transition between two hyperfine levels of the cesium-133 atom ground state. The currently operating fountain-type elementary cesium frequency standards are used to define the second from the corresponding microwave transition ( $\approx 9.2$  GHz). They have an accuracy of  $3 \times 10^{-16}$  and long-term stability of the order of  $10^{-15}$  per day [64]. In the nearest future, it will be possible to reach the accuracy level of  $1 \times 10^{-16}$  by using cryogenic technologies and taking systematic errors into account [65]. However, this level of accuracy is believed to be the limit for the cesium fountain. Despite such outstanding characteristics, this makes it impossible to perform many fundamental physical experiments and limits the practical applications of frequency and time metrology in the fields of precise navigation on Earth or in space, relativistic geodesy, and telecommunication technologies.

One revolutionary achievement on the way towards the transition to a new type of optical frequency standards was

made in 1999. It was the development of a new femtosecond laser with self-synchronization of modes of the ‘clock mechanism’ (optical and radio frequency synthesizer), which universally links any of its components to the reference frequency standard in the optical or microwave region [66–68]. Until that time, the problem of linking fast (uncountable) optical oscillations with electronically countable microwave oscillations remained largely unsolved.

The usual approach to solving this problem consists in creating frequency chains that link the center of the transition between components of the cesium atom hyperfine structure with some specific frequency in the optical range. Every link in these chains uses a nonlinear diode or crystal, and all intermediate oscillators at every stage must be phase-matched [3]. Linking frequency chains assembled in a number of laboratories was very complicated and required large material resources for their development and maintenance. But the main disadvantage of this approach was its experimental limit: each chain could measure only one specific frequency.

A qualitatively new stage in solving the problem of creating a ‘clock mechanism’ that would link the optical and microwave ranges began after the development of high-stability femtosecond lasers operating in the mode synchronization regime. The idea of using a laser with mode synchronization producing an equidistant frequency comb in order to measure frequency intervals (i.e., as a ‘frequency counter’) was independently proposed in the 1970s by Chebotayev together with Baklanov [69] and by Hansch and coauthors [70]. Only after many years was the true significance of this prophetic idea understood, when lasers with short enough femtosecond pulses were developed [67, 68]. Precisely this achievement—the development of a reliable clock mechanism that would link optical and microwave ranges—was awarded the Nobel prize in 2005. In their Nobel lectures, Hall and Hansch [67, 68] emphasized the pioneering contribution of Chebotayev to the idea of using lasers as frequency counters.

In the case of frequency standards based on neutral atoms, the decisive factor was a fruitful idea of Katori [44, 45] about the localization of ultracold atoms in spatial structures created by a laser standing wave (optical lattices). By choosing a specific wavelength of laser radiation (the so-called magic wavelength), the exact equality of quadratic Stark shifts can be achieved for the ground and excited states, which in turn fully compensates the shift of the reference optical resonance frequency, which is linear in intensity (‘light shift cancelation’ technique).

We note that the development of next-generation optical standards for frequency and time with a precision higher than that of the modern fountain-type cesium standards not only can open possibilities for performing new fundamental physical experiments but also is of unique practical interest for optical communication, navigation, and global positioning systems. The enormous, explosive interest in this problem that has occurred over recent years can easily be explained. Due to the high relevance and significance of this research field, there are numerous review articles, among which we mention out only the latest and, possibly, the most comprehensive one [71]. This allows us to further concentrate only on those new methods that were proposed, developed, and investigated by us in order to improve the stability and increase the accuracy of modern optical frequency standards.

## 2. Method of magnetically induced spectroscopy of strongly forbidden optical transitions

The first scheme of optical lattice clocks was proposed for odd isotopes [43, 44], which provide a reasonable width (of the order of several mHz) of the forbidden transition level due to the mixing of working levels  $^3P_0$  and  $^3P_1$  via a nonzero nuclear spin. Soon, such a scheme was experimentally realized for  $^{87}\text{Sr}$  by Japanese scientists [46, 51] and then successfully confirmed in other laboratories [52, 53]. But for odd isotopes, the energy levels are defined by the total angular momentum operator

$$\hat{\mathbf{F}} = \hat{\mathbf{S}}_n + \hat{\mathbf{J}}, \quad (2)$$

where  $\hat{\mathbf{S}}_n$  is the nuclear spin operator and  $\hat{\mathbf{J}} = \hat{\mathbf{L}} + \hat{\mathbf{S}}$  is the electron angular momentum operator ( $\hat{\mathbf{L}}$  and  $\hat{\mathbf{S}}$  are operators of orbital and spin momenta). In this case, the electronic transition  $^1S_0 \leftrightarrow ^3P_0$  transforms into the transition  $F_g = S_n \leftrightarrow F_e = S_n$  (Fig. 1), where  $F_{g,e}$  are total angular momenta of the ground and excited states, which are equal to the nuclear spin  $S_n$ . This means that the energy levels are degenerate with respect to the total angular momentum projection  $m$  ( $-S_n \leq m \leq S_n$ ). The energy shifts of the ground state sublevels  $|F_g, m\rangle$  in a magnetic field are determined only by the nuclear magneton, while the shifts of the magnetic sublevels of the upper state  $|F_e, m\rangle$  are determined by both nuclear and electronic magnetons (due to mixing with the magnetically sensitive state  $^3P_1$ ) (see Fig. 1). Therefore, g-factors of the ground and excited states are different, which in turn leads to a linear sensitivity of the transition frequency between magnetic sublevels to the magnetic field (see Fig. 1).

The clock transition in the case of odd isotopes is usually the one between Zeeman sublevels with the maximal magnetic quantum number  $m = S_n$ , which has the frequency shift  $\Delta g S_n \mu_B |\mathbf{B}|$ , where  $\mu_B$  is the Bohr magneton and  $\mathbf{B}$  is the magnetic field vector. As the estimates and experiments show, in order to provide the frequency standard stability on the level of  $10^{-17} - 10^{-18}$ , the magnetic field has to be controlled on the level of several  $\mu\text{G}$ , which is a quite difficult task.

We also note that the degeneracy of energy levels in odd isotopes (with respect to magnetic sublevels) leads to optical pump effects, which should also be taken into account when

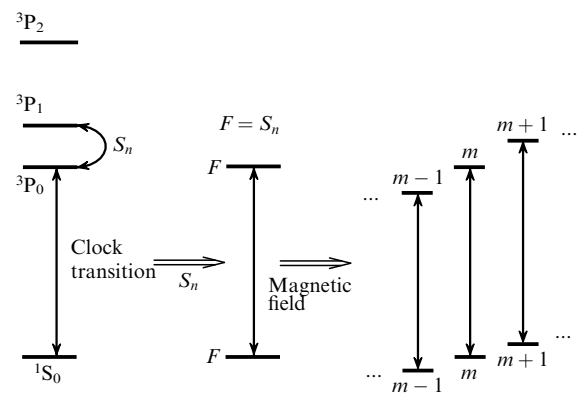


**Figure 1.** Schematic illustrating the Zeeman structure that forms in odd isotopes with a nonzero nuclear spin ( $S_n \neq 0$ ), and the linear sensitivity to the magnetic field of the frequency of optical transitions between Zeeman sublevels with the same magnetic quantum number  $m$  (due to different g-factors of upper and lower states).

determining the metrological characteristics of the frequency standards.

Therefore, even isotopes (those with the zero nuclear spin) that have nondegenerate energy states  $^1S_0$  and  $^3P_0$  are more suitable from the metrological standpoint, because in this case the frequency of the transition  $^1S_0 \leftrightarrow ^3P_0$  is not linearly sensitive to the magnetic field, and the optical pump effects are absent. However, the use of even isotopes encounters a profound problem: the transition  $^1S_0 \leftrightarrow ^3P_0$  is extremely weak and the reference resonance cannot be detected by using the standard single-photon excitation scheme. The idea of using two-photon [72, 73] and even three-photon [74] excitation schemes (with phase-matched lasers at significantly different frequencies) remains unrealized.

In this situation, we have proposed the method of magneto-induced excitation of forbidden transitions  $^1S_0 \leftrightarrow ^3P_0$  for even isotopes with zero nuclear spin [75]. The idea of this method is to use an external static magnetic field in order to mix the states  $^3P_0$  and  $^3P_1$ , which makes the transition  $^1S_0 \leftrightarrow ^3P_0$  partially allowed and enables its single-photon excitation.

We first consider a three-level system, illustrated in Fig. 2. We assume that states  $|1\rangle$  and  $|3\rangle$  have opposite parities, and an electric-dipole transition is possible between them, while states  $|2\rangle$  and  $|3\rangle$ , having the same parity, are connected through the magnetic-dipole transition. The transition between states  $|1\rangle$  and  $|2\rangle$  is assumed to be forbidden due to some selection rule (for example, by the total angular momentum). States  $|1\rangle$  and  $|2\rangle$  are long-lived, and in the framework of this model, their relaxation rate is zero. State  $|3\rangle$  has some nonzero relaxation rate  $\gamma$  due to the spontaneous transition  $|3\rangle \leftrightarrow |2\rangle$ .

We propose exciting the transition  $|1\rangle \leftrightarrow |2\rangle$  at a frequency  $\omega_{21}$  by simultaneously applying two fields. One of these fields is an optical probe with a frequency  $\omega_p$  and an amplitude  $E_p$ , which acts on the electric dipole transition  $|1\rangle \leftrightarrow |3\rangle$ . The corresponding matrix element is the Rabi frequency  $\Omega_E = \langle 3 | (\hat{d}E_p) | 1 \rangle / \hbar$ , where  $\hat{d}$  is the electric dipole moment operator. The other field is a static magnetic field  $\mathbf{B}$ , which links states  $|2\rangle$  and  $|3\rangle$  via the magnetic-dipole transition with the corresponding matrix element  $\Omega_B = \langle 2 | \hat{V}_m | 3 \rangle / \hbar$  of the magnetic-dipole interaction operator

$$\hat{V}_m = -\hat{\mu}_B \mathbf{B}, \quad (3)$$

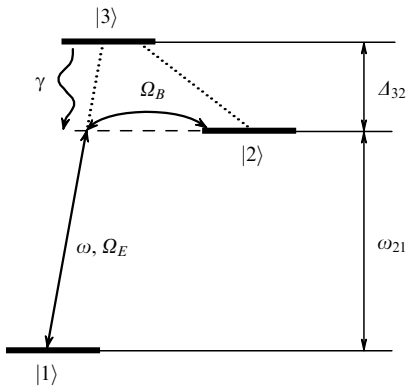


**Figure 2.** Three-level system illustrating the mechanism of magneto-induced resonance.

where  $\hat{\mu} = -\mu_B(\hat{\mathbf{J}} + \hat{\mathbf{S}})$  is the magnetic dipole momentum operator, defined by the operators the total  $\hat{\mathbf{J}}$  and spin  $\hat{\mathbf{S}}$  moments of the atom (in  $\hbar$  units). In this case, the Rabi frequency at the transition between states  $|1\rangle$  and  $|2\rangle$ , in the lowest approximation of the perturbation theory, has the form

$$V_{21} = \frac{\Omega_E \Omega_B}{\Delta_{32}}, \quad (4)$$

where  $\Delta_{32}$  is the difference between the frequencies of levels  $|3\rangle$  and  $|2\rangle$ . This means that as the probe field frequency  $\omega_p$  is scanned, a resonance must be observed at  $\omega_p = \omega_{21}$ , where  $\omega_{21}$  is the frequency of the forbidden transition  $|1\rangle \leftrightarrow |2\rangle$ .

This result can be explained in two ways. One interpretation is connected with the concept of mixing states  $|2\rangle$  and  $|3\rangle$ . Indeed, according to the first order of the perturbation theory (with respect to the parameter  $\Omega_B/\Delta_{32} \ll 1$ ), in the presence of a static magnetic field, state  $|2\rangle$  acquires a small admixture of state  $|3\rangle$ :

$$|2'\rangle = |2\rangle + \frac{\Omega_B}{\Delta_{32}} |3\rangle. \quad (5)$$

As a result, the transition  $|1\rangle \leftrightarrow |2'\rangle$  becomes partially allowed (for example, for spontaneous decay). We can use (5) to calculate Rabi frequency (4):  $V_{21} = \langle 2' | (\hat{d}E_p) | 1 \rangle / \hbar$ .

Another interpretation is in terms of two-photon spectroscopy. In this case, expression (4) can be considered a two-photon Rabi frequency in the limit where the frequency of one of the fields (in our case, the magnetic field) tends to zero. Then the frequency difference  $\Delta_{32}$  plays the role of a single-photon detuning, and the condition for the two-photon resonance corresponds to the equality of the optical field frequency and the forbidden transition frequency, i.e.,  $\omega = \omega_{21}$ .

We note that under the action of the applied fields, the frequency of the transition  $|1\rangle \leftrightarrow |2\rangle$  experiences quadratic shifts: an optical one

$$\Delta_E = \frac{|\Omega_E|^2}{4\Delta_{32}}, \quad (6)$$

and a magnetic one

$$\Delta_B = -\frac{|\Omega_B|^2}{\Delta_{32}}. \quad (7)$$

Expression (4) for the absolute value of  $V_{21}$  can then be rewritten as

$$|V_{21}| = 2\sqrt{|\Delta_E \Delta_B|}. \quad (8)$$

We can see from (8) that the same Rabi frequency can correspond to different values  $\Delta_E$  and  $\Delta_B$ . For example, if the magnetic field has higher stability, the more suitable situation (from the metrological standpoint) would be the one with a stronger magnetic shift component, and vice versa.

Moreover, the spontaneous transition line  $|2\rangle \leftrightarrow |1\rangle$  is broadened in accordance with the perturbation theory:

$$\gamma_{21} \approx \gamma \frac{|\Omega_B|^2}{\Delta_{32}^2}. \quad (9)$$

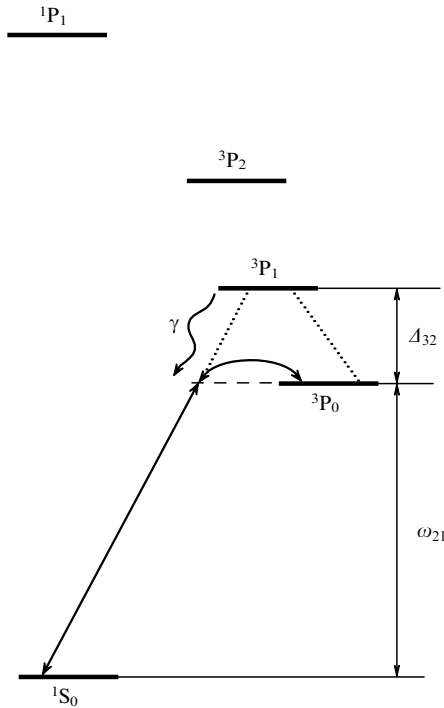


Figure 3. Level structure for alkali-earth atoms.

We see that the broadening is inversely proportional to the square of a large quantity  $\Delta_{32}$  and is therefore negligible in most cases.

Figure 3 shows a diagram of the main energy levels, which is typical for even isotopes of most alkali-earth atoms (Be, Mg, Ca, Sr, Zn, and Cd), mercury, and rare-earth ytterbium. Our goal is to excite the resonance corresponding to the forbidden transition  $^1S_0 \leftrightarrow ^3P_0$ .

State  $|1\rangle$  in Fig. 2 corresponds to the atomic state  $^1S_0$  and state  $|2\rangle$  corresponds to  $^3P_0$ . State  $|3\rangle$ , which provides the ‘two-photon’ linking, corresponds to  $^3P_1$ . In this scheme, the electric dipole interaction with the probe light field

$$\mathbf{E}_p(t) = \text{Re} \left\{ \mathbf{E}_p \exp [-i(\omega_p t - \mathbf{k}_p \mathbf{r})] \right\}, \quad \mathbf{E}_p = E_p \mathbf{e}_p, \quad (10)$$

is realized via the intercombination transition  $^1S_0 \leftrightarrow ^3P_1$ . Here,  $\mathbf{E}_p$  and  $E_p$  are vector and scalar amplitudes,  $\mathbf{e}_p$  is the unit polarization vector, and  $\mathbf{k}_p$  is the probe wave vector. Magnetic dipole interaction with the static magnetic field  $\mathbf{B}$  is realized via the transition  $^3P_1 \leftrightarrow ^3P_0$ .

With the vector nature of  $\mathbf{E}_p$  and  $\mathbf{B}$ , together with the Zeeman degeneracy of the state  $^3P_1$  taken into account, the expression for the total ‘magneto-induced’ Rabi frequency (4) takes the form

$$V_{21} = \frac{\sqrt{2}\mu_B \langle 3 || \hat{d} || 1 \rangle}{\sqrt{3} \hbar^2 \Delta_{32}} \mathbf{B} \mathbf{E}_p. \quad (11)$$

Here,  $\langle 3 || \hat{d} || 1 \rangle \equiv \langle ^3P_1 || \hat{d} || ^1S_0 \rangle$  is the reduced matrix element of the dipole moment for the transition  $^1S_0 \leftrightarrow ^3P_1$ , and its numerical value can be obtained empirically from the lifetime of the  $^3P_1$  state:

$$\frac{1}{\tau_{3P_1}} = \frac{4\omega_1^3 |\langle 3 || \hat{d} || 1 \rangle|^2}{3\hbar c^3},$$

where  $\omega_1$  is the frequency of the transition  $^1S_0 \leftrightarrow ^3P_1$ .

We now represent the magnetic field in the form  $\mathbf{B} = B\mathbf{b}$ , where the real unit vector  $\mathbf{b}$  ( $|\mathbf{b}| = 1$ ) describes the orientation of the vector  $\mathbf{B}$  and  $B = |\mathbf{B}|$ . In this case, expression (11) can be rewritten as

$$V_{21} = a\sqrt{I_p} B(\mathbf{b} \mathbf{e}_p) = a\sqrt{I_p} B \cos \varphi, \quad (12)$$

where  $I_p = c|\mathbf{E}_p|^2/(8\pi)$  is the intensity of the probe light wave, and the coefficient  $a$  is an individual characteristic of the chosen element;  $\varphi$  is the angle between the vectors  $\mathbf{b}$  and  $\mathbf{e}_p$  when the probe field is linearly polarized (that is, when  $\mathbf{e}_p^* = \mathbf{e}_p$ ). It is clear that the optimal orientation is the one where the vectors  $\mathbf{e}_p$  and  $\mathbf{b}$  are parallel and  $|\cos \varphi| = 1$ .

The quadratic Zeeman shift has the form

$$\Delta_B = bB^2, \quad (13)$$

and the light shift is expressed as

$$\Delta_E = wI_p, \quad (14)$$

where  $w$  is the dynamic polarizability at the transition frequency  $\omega_{21}$ . We note that in order to correctly calculate light shifts (14), the contributions of all states that are connected with the levels  $^3P_0$  and  $^1S_0$  by dipole transitions must be taken into account (for example, a contribution from the dipole transition with the level  $^1P_1$  in Fig. 3). Therefore, expression (8) for real atoms becomes

$$V_{21} = \chi \sqrt{|\Delta_E \Delta_B|}, \quad (15)$$

where  $\chi = a/\sqrt{|bw|} \neq 2$ .

We also note that besides the second-order paramagnetic interaction, which is responsible for shift (7) of the level  $^3P_0$ , a diamagnetic interaction makes its own contribution to the quadratic Zeeman effect (13), even in the first approximation:

$$\hat{V}_d = \frac{1}{8} [\mathbf{B} \times \mathbf{r}]^2 = \frac{B^2 r^2}{12} \left[ 1 - \sqrt{\frac{3}{2}} (\{\mathbf{b} \otimes \mathbf{b}\}_2 C_2(\theta, \varphi)) \right], \quad (16)$$

where  $\{\mathbf{b} \otimes \mathbf{b}\}_2$  is the second-rank tensor product of two vectors and  $C_{2m}(\theta, \varphi)$  is the modified spherical harmonic [76]. However, numerical calculations show that for all considered atoms, this contribution does not exceed 10% of the paramagnetic contribution.

As an example, we estimate the limit instability of the frequency in the framework of the proposed method for Yb atoms, based on realistic assumptions for the field values and their stability. For Yb, we use the values of the coefficients  $a \approx 18.6 \text{ mHz G}^{-1} (\text{mW cm}^{-2})^{-1/2}$ ,  $b \approx -62 \text{ mHz G}^{-2}$ ,  $w \approx 15 \text{ mHz (mW cm}^{-2})^{-1}$ , and  $\chi \approx 0.6$ . Modern experimental techniques allow obtaining a magnetic field  $|\mathbf{B}| = 10 \text{ G}$  with an uncertainty  $\sim 1 \text{ mG}$ . This leads to the regular quadratic shift  $\Delta_B = 6.2 \text{ Hz}$  with the uncertainty  $\delta(\Delta_B) \sim 1.2 \text{ mHz}$ . If  $I_p = 8 \text{ mW cm}^{-2}$ , the light shift is  $\Delta_E \approx 120 \text{ mHz}$ . If we use a realistic value for the intensity control at the level of 1%, the value of the possible light shift fluctuation is  $\delta(\Delta_E) \sim 1.2 \text{ mHz}$ . Then the frequency determination error can be estimated to be around 1.7 mHz, which means that the instability is of the order of  $3 \times 10^{-18}$  for the forbidden transition frequency  $5.183 \times 10^{14} \text{ Hz}$ . The Rabi frequency (12) for the field values mentioned above and for

$E_p \parallel \mathbf{B}$  is  $\tilde{\nu}_{12} \approx 0.5$  Hz. Stimulated transitions with such a Rabi frequency can be detected in atoms captured in a nondissipative optical lattice at the magic wavelength.

The estimates made for even Yb isotopes show that the described method is promising for application in new-generation optical frequency standards, which use atoms trapped in the optical lattice at the magic wavelength. In particular, the frequency instability can reach values  $10^{-17} - 10^{-18}$ , which are limited by the uncertainty of optical and quadratic Zeeman shifts. This method can be applied to alkali-earth atoms and to atoms with a similar energy level structure (Mg, Ca, Sr, Yb, Zn, Cd, Hg).

The magnetically induced spectroscopy method was successfully realized experimentally, first with  $^{174}\text{Yb}$  atoms [54, 56], then with  $^{88}\text{Sr}$  atoms [77–79], and recently with  $^{24}\text{Mg}$  atoms [80].

### 3. Generalized Ramsey method in ultra-high resolution spectroscopy of ultracold atoms and ions

As a specific example, we consider the magnetically induced spectroscopy method [75] described in Section 2, for the strictly forbidden optical transition  $^1S_0 \rightarrow ^3P_0$  in even isotopes of alkali-earth-type atoms trapped in an optical lattice at a magic wavelength. To be specific, we assume that the clock transition frequency  $\omega_0$  (in the presence of only the lattice field, including thermal and collision shifts) is unperturbed. In this case, the frequency shift

$$\Delta = \kappa I_p + \beta |\mathbf{B}|^2 \quad (17)$$

occurs, caused by the probe laser field (with the intensity  $I_p$ ) and a static magnetic field  $\mathbf{B}$  (see [75]).

When developing frequency standards (especially primary ones), an obvious question arises: “What should one do with these shifts?” We see two possible answers to this question. The first is in the precise experimental measurement of the coefficients  $\kappa$  and  $\beta$  with a high control rate over the values  $I_p$  and  $|\mathbf{B}|$ . Then, based on the results of spectroscopic measurements, we can calculate the unperturbed transition frequency  $\omega_0$  for  $I_p = 0$  and  $B = 0$ . For example, in the magnetic field  $B \sim 10^{-3}$  T ( $\sim 10$  G), the quadratic shift  $\beta |\mathbf{B}|^2$  is of the order of 10 Hz. In this case, in order to be able to reach absolute precision in the frequency determination at the level of 1 mHz and less (with a relative error less than  $10^{-17}$ ), we need to determine the value of the coefficient  $\beta$  and control the value of the magnetic field with an accuracy of  $10^{-4}$  (for the magnetic field, this corresponds to the order of 1 mG). Obviously, reaching such a level of precision for the measurement of the coefficient  $\beta$  would require great effort on the part of scientists over many years. Moreover, there is not much hope for theoretical calculations for many-electron atoms to have such an accuracy (that is, around 0.01%), due to the diamagnetic contribution. Similar estimations can be made for the shift caused by the probe laser field ( $\kappa I_p$ ).

In [81], we proposed a new solution to the problem of field shift (17). The suggested solution uses the Ramsey spectroscopy method with pulses separated in time (Fig. 4) with different durations. Speaking of magnetically induced spectroscopy [75], we here mean that during the action of the pulses (with the Rabi frequency  $\Omega_0$  and durations  $\tau_1$  and  $\tau_2$ ), the atoms are influenced by the probe laser field with a frequency  $\omega$  in the presence of the magnetic field  $\mathbf{B}$ , and

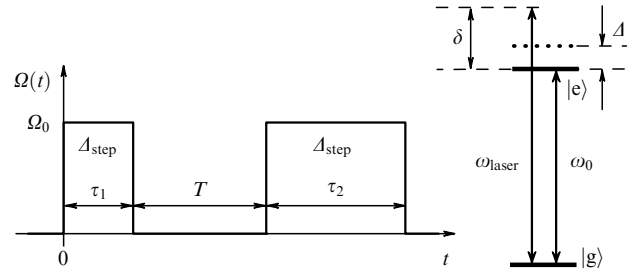


**Figure 4.** Illustration of Ramsey pulses with different durations ( $\tau_1$  and  $\tau_2$ ). During the action of Ramsey pulses, a frequency shift  $\Delta$  occurs.

during the free evolution (duration  $T$ ), the magnetic field and the probe wave are switched off simultaneously.

This means that the proposed scheme of Ramsey spectroscopy has one distinctive feature, which is related to the frequency shift  $\Delta$  only during the action of the pulses. If the atoms at the initial instant  $t = 0$  were in the ground state  $|g\rangle$ , then after the action of two pulses, the population of atoms in the excited state  $|e\rangle$  is

$$n_e = \frac{\Omega_0^2}{\Omega^2} \left\{ \left[ \cos \frac{\delta T}{2} \sin \frac{\Omega(\tau_1 + \tau_2)}{2} - \frac{2(\delta - \Delta)}{\Omega} \sin \frac{\delta T}{2} \sin \frac{\Omega\tau_1}{2} \sin \frac{\Omega\tau_2}{2} \right]^2 + \sin^2 \frac{\delta T}{2} \sin^2 \frac{\Omega(\tau_1 - \tau_2)}{2} \right\}, \quad (18)$$

where  $\delta = \omega - \omega_0$  is the detuning of the probe field frequency from the frequency of an unperturbed transition (that is, during the free evolution between two Ramsey pulses), and  $\Omega = (\Omega_0^2 + (\delta - \Delta)^2)^{1/2}$  is the generalized Rabi frequency during the action of the pulses.

Expression (18) describes Ramsey fringes, with the central resonance (as a function of  $\delta$ ) used as a reference one. The existence of an additional frequency shift  $\Delta$  during the action of the pulses also leads to a shift of the central resonance maximum  $\bar{\delta}\omega_0$  with respect to the frequency  $\omega_0$  of the unperturbed transition.

We describe the functional dependence of  $\bar{\delta}\omega_0$  under the condition  $|\Delta/\Omega_0| \ll 1$ . For this, we use the most general mathematical considerations and represent signal (18) as a Taylor series in the detuning  $\delta$ :

$$n_e = A^{(0)} + A^{(1)}\delta + A^{(2)}\delta^2 + \dots, \quad (19)$$

where the coefficients  $A^{(j)}$  can in turn be expanded in series in  $\Delta/\Omega_0$  as

$$\begin{aligned} A^{(0)} &= \mathcal{A}_0^{(0)} + \mathcal{A}_2^{(0)} \left( \frac{\Delta}{\Omega_0} \right)^2 + \mathcal{A}_4^{(0)} \left( \frac{\Delta}{\Omega_0} \right)^4 + \dots, \\ A^{(1)} &= \mathcal{A}_1^{(1)} \left( \frac{\Delta}{\Omega_0} \right) + \mathcal{A}_3^{(1)} \left( \frac{\Delta}{\Omega_0} \right)^3 + \dots, \\ A^{(2)} &= \mathcal{A}_0^{(2)} + \mathcal{A}_2^{(2)} \left( \frac{\Delta}{\Omega_0} \right)^2 + \mathcal{A}_4^{(2)} \left( \frac{\Delta}{\Omega_0} \right)^4 + \dots, \end{aligned} \quad (20)$$

This result directly follows from the symmetry of expression (18) under the transformation  $\delta \rightarrow -\delta$ ,  $\Delta \rightarrow -\Delta$ .

If  $|A/\Omega_0| \ll 1$ , we can use expression (19) to easily find the sought  $\overline{\delta\omega_0}$  in the form

$$\overline{\delta\omega_0} \approx -\frac{A^{(1)}}{2A^{(2)}}. \quad (21)$$

Relation (21), together with (20), allows us to determine the main part of the dependence of  $\overline{\delta\omega_0}$  on  $A/\Omega_0$ . For example, in the case of Ramsey pulses with equal duration ( $\tau_1 = \tau_2 = \tau$ ), this dependence is linear:

$$\overline{\delta\omega_0} \propto \frac{A}{\Omega_0}. \quad (22)$$

But as we show below, this formula is inapplicable in the general case of Ramsey pulses with different durations ( $\tau_1 \neq \tau_2$ ). In particular, by choosing special values of the parameters ( $\tau_1, \tau_2, \Omega_0$ ) for  $|A/\Omega_0| \ll 1$ , we can obtain a cubic dependence:

$$\overline{\delta\omega_0} \propto \left(\frac{A}{\Omega_0}\right)^3. \quad (23)$$

This allows drastically improving the metrological characteristics of atomic clocks based on the Ramsey spectroscopy method over that in the case of the single-pulse method (Rabi spectroscopy), which is used today in optical atomic clocks.

For these purposes, we consider the expression for the coefficient  $\mathcal{A}_1^{(1)}$  in (20):

$$\begin{aligned} \mathcal{A}_1^{(1)} &= \frac{\sin[\Omega_0(\tau_1 + \tau_2)/2]}{\Omega_0} \\ &\times \left[ 2 \sin \frac{\Omega_0(\tau_1 + \tau_2)}{2} + 2\Omega_0 T \sin \frac{\Omega_0 \tau_1}{2} \sin \frac{\Omega_0 \tau_2}{2} \right. \\ &\left. - \Omega_0(\tau_1 + \tau_2) \cos \frac{\Omega_0(\tau_1 + \tau_2)}{2} \right]. \end{aligned} \quad (24)$$

It follows that if the condition

$$\Omega_0(\tau_1 + \tau_2) = 2\pi n, \quad n = 1, 2, 3, \dots \quad (25)$$

holds, then  $\mathcal{A}_1^{(1)} = 0$ , which, according to (20) and (21), leads to the cubic leading dependence of  $\overline{\delta\omega_0}$  on  $A/\Omega_0$  in (23).

However, for the application to optical clocks, besides condition (25), which significantly decreases the shift  $\overline{\delta\omega_0}$ , we also need the amplitude of the central resonance to be close to maximal. Notably, this can be achieved by maximizing the coefficient  $\mathcal{A}_0^{(2)}$  in (20), which determines the curvature of the central resonance peak under the condition  $|A/\Omega_0| \ll 1$ . It can be shown that under condition (25), the relation

$$\mathcal{A}_0^{(2)} = \frac{T^2}{4} \sin^2(\Omega_0 \tau_1) \quad (26)$$

holds, which implies that the coefficient  $\mathcal{A}_0^{(2)}$  reaches its maximal value at

$$\Omega_0 \tau_1 = \frac{\pi(2m+1)}{2}, \quad m = 0, 1, 2, \dots \quad (27)$$

Combining conditions (25) and (27) leads to the following relation for  $\tau_1$  and  $\tau_2$ :

$$\frac{\tau_2}{\tau_1} = \frac{4n}{2m+1} - 1. \quad (28)$$

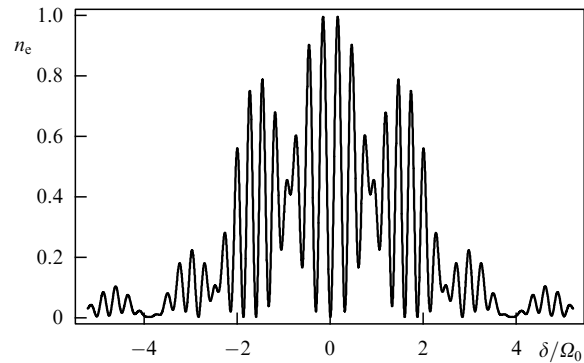
In the simplest case  $n = 1$  [that is, in the case where  $\Omega_0(\tau_1 + \tau_2) = 2\pi$  in (25)], we obtain  $\tau_2/\tau_1 = 3$  (for  $m = 0$ ) or  $\tau_2/\tau_1 = 1/3$  (for  $m = 1$ ), i.e., one of the Ramsey pulses is one third the length of the other. Figure 5 shows the total Ramsey pattern in this case and Fig. 6 shows the curve of the central resonance, together with that for the standard Ramsey method with equal pulses ( $\Omega_0 \tau_1 = \Omega_0 \tau_2 = \pi/2$ ). As can be seen, the amplitude of the resonance in our method is also close to the maximal value ( $\approx 1$ ).

We note that the difference in pulse durations ( $\tau_2 \neq \tau_1$ ) is a principle feature of the proposed method. Indeed, if equal pulses are used ( $\tau_2 = \tau_1$ ) when condition (25) is satisfied, then the central resonance has a flat peak and small amplitude, which is unsuitable for optical standards.

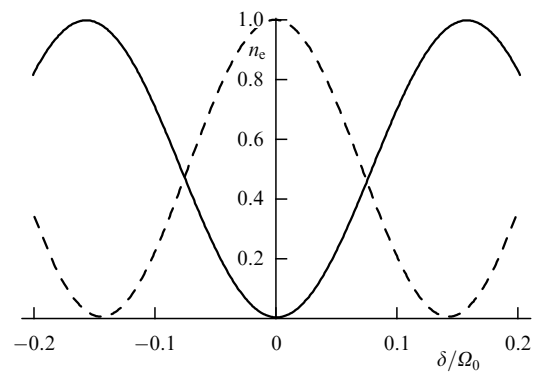
We now consider the dependence of the shift  $\overline{\delta\omega_0}$  on  $A/\Omega_0$  in more detail. Figure 7a clearly proves the general considerations discussed above, according to which the fulfillment of condition (25) leads to a drastic decrease in the central resonance shift sensitivity (for  $|A/\Omega_0| \ll 1$ ), in contrast to the case of standard Ramsey spectroscopy with equal pulses (Fig. 7b).

Figure 8 shows the emergence of a linear contribution (in  $A/\Omega_0$ ) under the condition  $\Omega_0(\tau_1 + \tau_2) \neq 2\pi$ . The slope of this linear contribution is positive if  $\Omega_0(\tau_1 + \tau_2) > 2\pi$  and negative if  $\Omega_0(\tau_1 + \tau_2) < 2\pi$ .

To demonstrate the effectiveness of the new method, we use quite realistic estimates for the control rate of  $\Omega_0(\tau_1 + \tau_2)$ ,



**Figure 5.** Ramsey fringes with condition (25) satisfied:  $\Omega_0(\tau_1 + \tau_2) = 2\pi$ ,  $\tau_2/\tau_1 = 3$ ,  $\Omega_0 T = 20$ ,  $A = 0$ ;  $n_e$  is the population of the excited state.



**Figure 6.** Comparison of central Ramsey resonances with condition (25) satisfied ( $\Omega_0(\tau_1 + \tau_2) = 2\pi$ ,  $\tau_2/\tau_1 = 3$ ,  $\Omega_0 T = 20$ ,  $A = 0$ ) (solid curve) and in the case of standard Ramsey spectroscopy with equal pulses ( $\Omega_0 \tau_1 = \Omega_0 \tau_2 = \pi/2$ ,  $\Omega_0 T = 20$ ,  $A = 0$ ) (dashed curve).

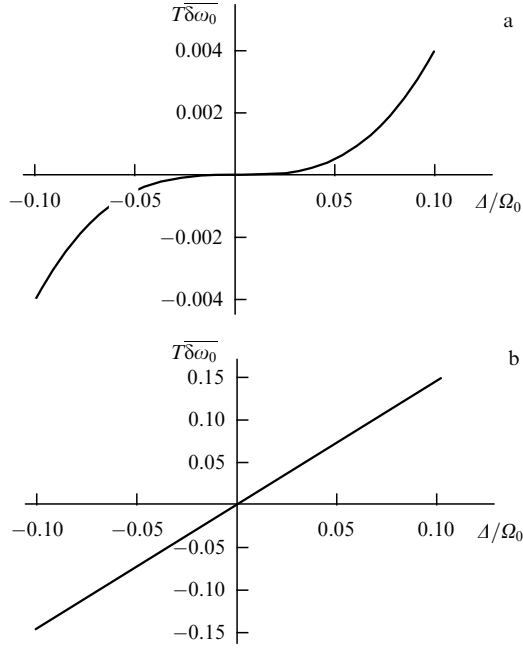


**Figure 7.** Numerical calculation results for the central resonance shift  $T\bar{\delta}\omega_0$  dependence on  $\Delta/\Omega_0$ : (a) for a new type of Ramsey spectroscopy under the fulfillment of condition (25) ( $\Omega_0(\tau_1 + \tau_2) = 2\pi$ ,  $\tau_2/\tau_1 = 3$ ,  $\Omega_0 T = 20$ ), (b) for the standard Ramsey spectroscopy with equal pulses ( $\Omega_0\tau_1 = \Omega_0\tau_2 = \pi/2$ ;  $\Omega_0 T = 20$ ).

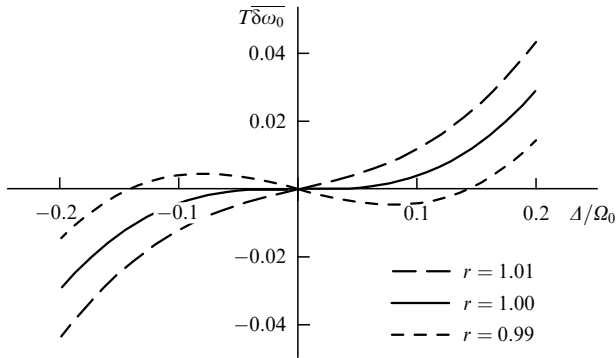


**Figure 8.** Numerical calculation results for the central resonance shift  $T\bar{\delta}\omega_0$  dependence on  $\Delta/\Omega_0$  for different values of the parameter  $r = \Omega_0(\tau_1 + \tau_2)/(2\pi)$  ( $\tau_2/\tau_1 = 3$  and  $\Omega_0 T = 20$ ).

the level of a 1% offset from  $2\pi$ , and  $|\Delta/\Omega_0| < 0.01$ . In this case,  $|\bar{\delta}\omega_0| < 0.00075/T$  (in  $\text{s}^{-1}$  units) for  $\Omega_0 T = 20$ . For example, if we set  $T = 0.5$  s (that is,  $\Omega_0 \approx 6.4$  Hz, which can be realized in the magnetically induced spectroscopy method in modern standards based on atoms in an optical lattice [54, 77]), then we obtain the estimate  $|\bar{\delta}\omega_0| < 0.0003$  Hz, which corresponds to a relative frequency uncertainty lower than  $10^{-18}$ . For comparison, if we consider the standard Ramsey method with equal pulses ( $\Omega_0\tau_1 = \Omega_0\tau_2 = \pi/2$ ) under the same conditions ( $|\Delta/\Omega_0| < 0.01$ ,  $\Omega_0 T = 20$ ), we obtain  $|\bar{\delta}\omega_0| < 0.015/T$ , which is more than one order of magnitude (in this case, 20 times) larger than in our method.

The proposed method was experimentally realized at Physikalisch-Technische Bundesanstalt (PTB) (Brunswick, Germany) [82] under our careful supervision of the experiment. The frequency field shift was suppressed by more than three orders of magnitude. Recently, a successful experimen-

tal realization of the combination of two of our methods — magnetically induced spectroscopy and generalized Ramsey spectroscopy — was reported in [79]. Further generalizations of the proposed method, which include taking the finite line width of the laser radiation and the lifetime of the excited state into account, can be found in our papers [83, 84].

#### 4. Synthetic frequency method

Two of the main factors that limit the accuracy of modern atomic frequency and time standards are the thermal shift and its temperature fluctuations. A happy exception is the  $^{27}\text{Al}^+$  ion [40, 43, 47] (and possibly  $^{115}\text{In}^+$  [85]), for which the polarizabilities of the upper and lower levels of the clock transition  $^1S_0 \rightarrow ^3P_0$  luckily coincide with quite a high accuracy. As a result, the thermal shift of the mentioned optical transition in  $^{27}\text{Al}^+$  at room temperature has a relative value slightly less than  $10^{-17}$ , while in all other atomic standards, this value is much higher. For example, in the case of the quadrupole transition  $^2S_{1/2} \rightarrow ^2D_{3/2}$  in the  $^{171}\text{Yb}^+$  ion, the relative thermal shift at room temperature is  $5.8 \times 10^{-16}$  [86]. For modern lattice clocks with strontium [55, 87] and ytterbium [54, 88], the respective thermal shifts (at the  $^1S_0 \rightarrow ^3P_0$  transition) are  $5.5 \times 10^{-15}$  and  $2.5 \times 10^{-15}$  [89]. In the case of the cesium radio frequency standard, this value is  $2.12 \times 10^{-14}$  [90].

Currently, there are two solutions to the thermal shift problem. A radical approach is based on the use of cryogenic technologies in order to make this shift negligible. Up to now, this method has been implemented only for mercury ions  $^{199}\text{Hg}^+$  [39]. Another approach involves precise thermal stabilization of the setup (in order to decrease the influence of temperature fluctuations) together with numerical calculations (theoretical and/or semi-empirical) of the shift at a given temperature.

In [91], we proposed an alternative method, which allows significantly (by two to three orders of magnitude) decreasing the thermal shift and its fluctuations in atomic standards without using cryogenic technologies or precise thermal stabilization. Our approach is based on using two clock transitions placed in an identical thermodynamic environment. Such a system has a combination frequency that does not undergo a thermal shift even at room temperature.

Our method is based on the fact that in the majority of cases, the thermal shift has almost the same temperature dependence for different transitions in atoms and ions. This universal dependence is described as  $\Delta_T \propto T^4$ .

We now consider two clock transitions with frequencies  $\omega_1^{(0)}$  and  $\omega_2^{(0)}$  in the same thermodynamic environments, that is, in the same cell. For definiteness, we assume that  $\omega_1^{(0)} < \omega_2^{(0)}$ . Then the frequency of each transition with the thermal shift taken into account can be represented as

$$\omega_j(T) = \omega_j^{(0)} + a_j T^4, \quad j = 1, 2, \quad (29)$$

where  $a_j$  is an individual characteristic of the  $j$ th transition, which depends on the atomic structure;  $a_j$  is mostly determined by the scalar part of the polarizability tensor in the static electric field. We introduce the coefficient  $\alpha_{12} = a_1/a_2$ . It is easy to see that the superposition  $\omega_1(T) - \alpha_{12}\omega_2(T)$  does not experience a thermal shift:

$$\omega_1(T) - \alpha_{12}\omega_2(T) = \omega_1^{(0)} - \alpha_{12}\omega_2^{(0)}. \quad (30)$$



We can now define a new ‘synthetic’ frequency  $\omega_{\text{synt}}$  as

$$\omega_{\text{synt}} = K(\omega_1(T) - \alpha_{12}\omega_2(T)) = K(\omega_1^{(0)} - \alpha_{12}\omega_2^{(0)}), \quad (31)$$

where  $K$  is some numerical factor, which is random in general. If some technology allowed the use of the frequency  $\omega_{\text{synt}}$  as a reference one, then we would be able to create atomic clocks where the thermal shift and its temperature fluctuations are suppressed, even at room temperature. At the same time, the thermal shifts  $a_j T^4$  at operating frequencies  $\omega_j$  can be rather large.

We show that such a practical application can be realized by using a femtosecond frequency synthesizer. We consider a situation where the frequency synthesizer is stabilized by two frequencies  $\omega_1(T)$  and  $\omega_2(T)$  at a fixed temperature  $T$  (Fig. 9). As a result, the parameters of a femtosecond comb can be uniquely defined as

$$\begin{aligned} d &= \frac{\omega_2(T) - \omega_1(T)}{n_2 - n_1} = \frac{\omega_2^{(0)} - \omega_1^{(0)}}{n_2 - n_1} + \frac{a_2 - a_1}{n_2 - n_1} T^4, \\ f_0 &= \omega_1(T) - n_1 d \\ &= \frac{n_2 \omega_1^{(0)} - n_1 \omega_2^{(0)}}{n_2 - n_1} + \frac{n_2 a_1 - n_1 a_2}{n_2 - n_1} T^4, \end{aligned} \quad (32)$$

where  $d$  is the pulse repetition rate,  $f_0$  the offset frequency, and  $n_1$  and  $n_2$  are fixed integers. Then the frequency of the  $m$ th mode is

$$\begin{aligned} \omega_m(T) &= f_0 + m d \\ &= \frac{m(\omega_2^{(0)} - \omega_1^{(0)}) + n_2 \omega_1^{(0)} - n_1 \omega_2^{(0)}}{n_2 - n_1} \\ &\quad + \frac{m(a_2 - a_1) + n_2 a_1 - n_1 a_2}{n_2 - n_1} T^4. \end{aligned} \quad (33)$$

From (33), we can obtain the value  $m = m_0$  at which the  $T^4$  term vanishes:

$$m_0 = \frac{n_1 a_2 - n_2 a_1}{a_2 - a_1} = \frac{n_1 - \alpha_{12} n_2}{1 - \alpha_{12}}. \quad (34)$$

In this case, the thermal shift for the frequency  $\omega_{m_0}$  is suppressed. After some simple mathematical transformations, we conclude that  $\omega_{m_0}$  is synthetic frequency (31),

$$\omega_{m_0} = \omega_{\text{synt}}^{\text{comb}} = \frac{\omega_1^{(0)} - \alpha_{12} \omega_2^{(0)}}{1 - \alpha_{12}}, \quad (35)$$

as could be expected. It is obvious that by  $m_0$ , we mean the integer that is nearest to the right-hand side of (34). More-

over, the requirement  $m_0 > 0$  must hold, which is equivalent to  $\omega_{\text{synt}}^{\text{comb}} > 0$  in (35).

We have shown that in a frequency comb stabilized by two clock transitions ( $\omega_1^{(0)}$  and  $\omega_2^{(0)}$ ), there is a frequency component (for  $m_0 > 0$ ) for which the thermal shift and sensitivity to temperature fluctuations are significantly suppressed. This frequency component can play the role of an atomic frequency standard. Moreover, from the practical standpoint, there can be a whole frequency band with suppressed thermal shift. Indeed, the frequency components that are nearest to  $\omega_{m_0}$ ,  $\omega_{m_0 \pm q}$  (with relatively small  $q$ ),

$$\omega_{m_0 \pm q} = \omega_{m_0} \pm q d = \omega_{m_0} \pm q \frac{\omega_2^{(0)} - \omega_1^{(0)}}{n_2 - n_1} \pm q \frac{a_2 - a_1}{n_2 - n_1} T^4, \quad (36)$$

also have a very low sensitivity to the thermal shift if  $n_2 - n_1 \gg 1$ . For example, in the case of optical frequencies  $\omega_1^{(0)}$  and  $\omega_2^{(0)}$ ,  $n_2 - n_1$  can reach several tens or hundreds of thousands (see the example below for the  $^{171}\text{Yb}^+$  ion). Because the exact value of the coefficient  $\alpha_{12}$  cannot be determined, there is some arbitrariness in the choice of the  $m_0$ th harmonic. This arbitrary choice is also caused by the principal limitation of our method, which is connected with higher-order corrections in  $T$  to the temperature dependence of the thermal shift:

$$\Delta_T^{(j)} = a_j T^4 + b_j T^6 + c_j T^8 + \dots, \quad j = 1, 2. \quad (37)$$

Usually, at room temperature, these corrections ( $b_j T^6 + c_j T^8 + \dots$ ) amount to  $\sim 0.01$ – $0.001$  of the dominant term  $a_j T^4$ . Hence, there is not much use in suppressing the dependence  $\propto T^4$  in our method by more than two to three orders of magnitude, because the residual thermal shift would not be decreased any more. In other words, in order to determine the range of suitable values of  $m_0$ , it suffices to obtain the value of  $\alpha_{12}$  with a relative accuracy  $\sim 0.01$ – $0.001$ . The chosen frequency harmonic  $\omega_{m_0}$  could be considered a universal atomic standard if there were agreement among laboratories on the fixed values of two integers:  $n_2 - n_1$  and  $m_0$ .

We note that the frequency  $\omega_{m_0}$  can be derived not only from theoretical calculations but also from experiment. For this, we should use a low-frequency electric field (or infrared laser) and find the static polarizabilities at clock transitions  $\omega_1$  and  $\omega_2$ . Furthermore, it is very convenient from the practical standpoint that there is no difference between the values of the electric field, because the needed coefficient  $\alpha_{12}$  equals the ratio of the scalar parts of unknown polarizabilities. Moreover, in the case of a comb generator stabilized by  $\omega_1$  and  $\omega_2$ , the frequency  $\omega_{m_0}$  can be directly determined as the one that does not undergo a scalar Stark shift in the low-frequency field.

Besides the frequency  $\omega_{m_0}$  (which can refer to the optical range), a low-frequency signal can be found in our system:

$$\frac{\omega_{m_0}}{m_0} = d + \frac{f_0}{m_0}. \quad (38)$$

This signal corresponds to a standard at the frequency  $\omega_{m_0}$ . Indeed, because the parameters  $d$  and  $f_0$  of the frequency comb can be measured with high precision, we can use a real radio frequency  $d$  and constantly correct it with the numerical term  $f_0/m_0$ , such that superposition (38) becomes insensitive

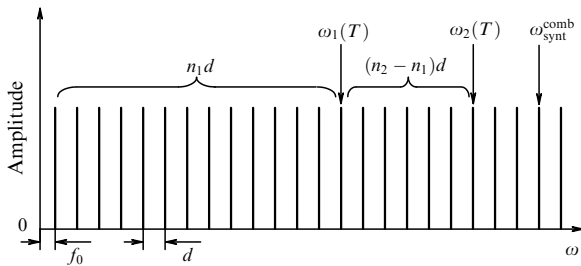


**Figure 9.** Illustration of a femtosecond frequency comb stabilized by two clock transitions with frequencies  $\omega_1$  and  $\omega_2$  at a fixed temperature  $T$ .

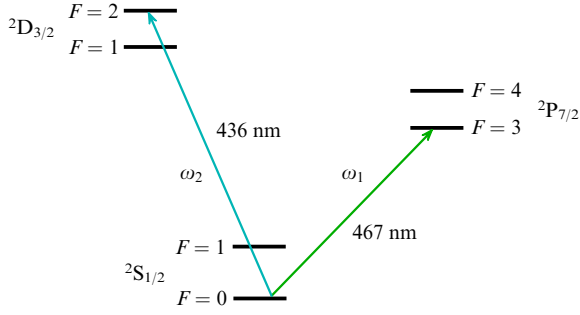


**Figure 10.** Hyperfine level structure and clock transitions used in the  $^{171}\text{Yb}^+$  ion.

to the thermal shift and corresponds to the standard at the frequency  $\omega_{m_0}$ . Interestingly, radio frequency (38) can be defined in our system even if  $m_0 < 0$  in (34), that is, if the primary frequency component  $\omega_{m_0} < 0$  and exists only virtually.

As a demonstrative example of the possible practical realization of the ideas presented above, we consider the  $^{171}\text{Yb}^+$  ion, where two clock transitions can be used (Fig. 10): the quadrupole transition  $^2\text{S}_{1/2} \rightarrow ^2\text{D}_{3/2}$  ( $F = 0 \rightarrow F = 2$ ,  $\lambda \approx 436$  nm) and the octupole transition  $^2\text{S}_{1/2} \rightarrow ^2\text{F}_{7/2}$  ( $F = 0 \rightarrow F = 3$ ,  $\lambda \approx 467$  nm). Detailed information on the spectroscopy of these transitions can be found in [92–94].

Using the results of polarizability calculations for the above transition, performed in [95] ( $\alpha_{12} \approx 0.382$ ), we obtain the synthetic frequency  $\omega_{\text{synt}}^{\text{comb}} \approx 614$  THz ( $\lambda_{\text{synt}} \approx 488$  nm). As we can see, this frequency is quite close to the frequencies of initial clock transitions (436 and 467 nm), and it can actually be present in the spectrum of the comb generator. The thermal shift is in this case suppressed by two orders of magnitude, down to the relative level of  $\sim 10^{-17}$  (or possibly even lower).

We can also estimate the frequency band (around  $\omega_{\text{synt}}^{\text{comb}}$ ) where all components of the frequency comb have a similar ( $\sim 10^{-2}$ ) level of suppression of the thermal shift and its temperature fluctuations. The width of this band is around 1 THz. This means that if we define  $d \approx 100$  MHz, then there are around  $10^4$  harmonics within the specified band and all of them can be chosen as a standard. We also note that for  $d \approx 100$  MHz, the number of harmonics between frequencies  $\omega_1$  and  $\omega_2$  can be estimated as  $n_2 - n_1 \sim 4.6 \times 10^5$ .

We analyze another possible realization of the synthetic frequency standard, which uses lattice clocks based on the transition  $^1\text{S}_0 \rightarrow ^3\text{P}_0$  in alkali-earth neutral atoms. For example, we consider strontium (wavelength  $\lambda \approx 698.4$  nm) and ytterbium ( $\lambda \approx 578.4$  nm). Using the calculation results in [89],  $\alpha_{12} \approx 1.69$ , the synthetic frequency can be estimated as  $\omega_{\text{synt}}^{\text{comb}} \approx 648$  THz ( $\lambda_{\text{synt}} \approx 463$  nm). However, the technical realization of such a scheme requires great effort because of the need to operate with lattice clocks for different atoms (strontium and ytterbium) situated in the same vacuum chamber.

From the technological standpoint, it is more suitable to use two different isotopes of the same element, for example,  $^{87}\text{Sr}$ – $^{88}\text{Sr}$  [87] and  $^{171}\text{Yb}$ – $^{174}\text{Yb}$  (or  $^{171}\text{Yb}$ – $^{173}\text{Yb}$ ) [54, 88]. However, we would then face a serious problem of determining the value and the sign of  $\omega_{\text{synt}}^{\text{comb}}$  in (35). This is because the conditions  $\omega_1 \approx \omega_2$  and  $\alpha_{12} \approx 1$  simultaneously hold in such systems, and expression (35) becomes extremely sensitive to a

very small quantity  $1 - \alpha_{12} \sim \pm 10^{-4} - 10^{-6}$ . Indeed, expression (35) can be represented as

$$\omega_{\text{synt}}^{\text{comb}} = \frac{\omega_1^{(0)} - \omega_2^{(0)}}{1 - \alpha_{12}} + \omega_2^{(0)}, \quad (39)$$

which shows that it is quite difficult to calculate the first term for isotopes with good accuracy. And although the isotopic shift  $\omega_1^{(0)} - \omega_2^{(0)}$  for the mentioned strontium and ytterbium isotopes is well measured [87, 88], high-precision calculations and/or experiments on deriving the polarizability for various isotopes have not yet been performed. Moreover, we can see from (39) that the sensitivity to other systematic shifts (for example, to the quadratic Zeeman shift) can be significantly increased (due to the small denominator  $1 - \alpha_{12}$ ), which can even cast doubt on the appropriateness of applying the discussed method in this case.

In order to see the full picture, we note that the idea of a synthetic frequency can be realized not only in the case of optical frequencies  $\omega_1$  and  $\omega_2$  but also, in principle, in the radio band, for example, by using the hyperfine splitting of an alkali-earth atom ground state, which is used in radio frequency standards (fountain clock). In that case, there must be a possibility of alternately working with two different atoms in the same setup in order to detect the corresponding radio frequency resonances. If this is possible, then, for example, a  $^{133}\text{Cs}$  and  $^{87}\text{Rb}$  pair can be considered.

We have proposed and developed the concept of an atomic frequency standard in which the thermal shift and its temperature fluctuations can be significantly suppressed (decreased by two to three orders of magnitude) even without using cryogenic technologies. This concept is based on the fact that in the system of two clock transitions with frequencies  $\omega_1$  and  $\omega_2$  placed in an identical thermodynamic environment, there is a frequency superposition  $\omega_{\text{synt}} \propto \omega_1 - \alpha_{12}\omega_2$  that is insensitive to the thermal shift  $\propto T^4$ . We define this superposition as the ‘synthetic’ frequency  $\omega_{\text{synt}}$ .

We propose a method for the practical realization of this idea by using a frequency comb generator stabilized by the original frequencies  $\omega_1$  and  $\omega_2$ . In this case, the frequency  $\omega_{\text{synt}}$  can exist as one of the frequency components of this generator, and it can be used as an atomic standard. We show in a specific example that, based on the  $^{171}\text{Yb}^+$  ion, we can develop optical clocks in which the relative thermal shift would be suppressed to the level of  $\sim 10^{-17}$  (or even lower), which is comparable with that for clocks based on the  $^{27}\text{Al}^+$  ion [40, 43, 47].

In addition, the obtained results will stimulate theoretical atomic calculations concerning the thermal shift. For example, we have to determine not only the polarizability but also higher-order corrections to the temperature dependence, that is,  $b_j T^6 + c_j T^8 + \dots$ , in (37) in order to obtain the principal limitation on the possible suppression of the thermal shift in our method.

## 5. Conclusions

We have presented three new methods for precise spectroscopy of ultracold atoms and ions, which were proposed, developed, and investigated at the Institute of Laser Physics, Siberian Branch, Russian Academy of Sciences (SB RAS). We note that experimental research on magnesium atoms and single ytterbium ions, which is aimed at the practical

realization of these methods, has been actively carried out at in the Institute since 2012. We plan to reach a level of relative instability better than  $10^{-16}$  by 2016.

In conclusion, we would like to make a forecast for the development of the research in the field of optical frequency standards:

(1) further improvement of metrological characteristics for ion ( $\text{Al}^+$ ,  $\text{Yb}^+$ ,  $\text{In}^+$ ,  $\text{Sr}^+$ ,  $\text{Hg}^+$ ) and atomic ( $\text{Sr}$ ,  $\text{Hg}$ ,  $\text{Yb}$ ,  $\text{Mg}$ ,  $\text{Tm}$ ) optical frequency standards by using special methods of control over the frequency field shifts of different natures (thermal radiation, trap and lattice fields, probe field); reaching the uncertainty level of  $10^{-18}$  in the nearest future; redefinition of frequency and time units based on optical frequency standards; precise verification of fundamental physical laws by using optical frequency standards;

(2) development of fundamentally new optical frequency standards (for example, based on nuclear transitions, magnetic dipole transitions in multicharged ions, etc.) that would allow reaching the frequency relative instability of the order of  $10^{-19}$  and lower;

(3) development of compact mobile optical frequency standards based on ultracold atoms and ions, including those working in space and used for high-precision navigation and geodesy systems;

(4) improvement of metrological characteristics of optical frequency standards by realizing quantum networks of atomic clocks and using fiber and space communication lines.

The studies presented in this paper were financially supported by the general committee of SB, RAS (integration project No. 62 “Precise spectroscopy of ultracold atoms: theory, mathematical modeling and experiment”), the Ministry of Education and Science of the Russian Federation (government contract 2014/139, project 826), the Russian Foundation for Basic Research (projects 15-02-08377, 15-32-20330, 14-02-0072, 14-02-00939), and a grant from the President of the Russian Federation (4096.2014.2). Experimental investigations with ultracold magnesium atoms and single ytterbium ions are respectively supported by the Russian Scientific Fund grants 16-12-0054 and 16-12-00052.

## References

- Letokhov V S, Chebotayev V P *Nonlinear Laser Spectroscopy* (Berlin: Springer-Verlag, 1977); Translated from Russian: *Printsipy Nelineinoi Lazernoi Spektroskopii* (Moscow: Nauka, 1975)
- Basov N G, Letokhov V S *Sov. Phys. Usp.* **11** 855 (1969); *Usp. Fiz. Nauk* **96** 585 (1968)
- Bagaev S N, Chebotaev V P *Sov. Phys. Usp.* **29** 82 (1986); *Usp. Fiz. Nauk* **148** 143 (1986)
- Letokhov V S, Chebotayev V P *Nelineinaya Lazernaya Spektroskopiya Sverkhvysokogo Razresheniya* (Nonlinear Laser Spectroscopy of Ultrahigh Resolution) (Moscow: Nauka, 1990)
- Letokhov V S *JETP Lett.* **7** 272 (1968); *Pis'ma Zh. Eksp. Teor. Fiz.* **7** 348 (1968)
- Balykin V I, Letokhov V S, Mishin V I *JETP Lett.* **29** 560 (1979); *Pis'ma Zh. Eksp. Teor. Fiz.* **29** 614 (1979)
- Andreev S V et al. *JETP Lett.* **34** 442 (1981); *Pis'ma Zh. Eksp. Teor. Fiz.* **34** 463 (1981)
- Dubetskii B Ya et al. *JETP Lett.* **39** 649 (1984); *Pis'ma Zh. Eksp. Teor. Fiz.* **39** 531 (1984)
- Kazantsev A P *Sov. Phys. Usp.* **21** 58 (1978); *Usp. Fiz. Nauk* **124** 113 (1978)
- Letokhov V S, Minogin V G *Phys. Rep.* **73** 1 (1981)
- Balykin V I, Letokhov V S, Minogin V G *Sov. Phys. Usp.* **28** 803 (1985); *Usp. Fiz. Nauk* **147** 117 (1985)
- Minogin V G, Letokhov V S *Laser Light Pressure on Atoms* (New York: Gordon and Breach Sci. Publ., 1987); Translated from Russian: *Davlenie Lazernogo Izlucheniya na Atomy* (Moscow: Nauka, 1986)
- Kazantsev A P, Surdutovich G I, Yakovlev V P *Mechanical Action of Light on Atoms* (Singapore: World Scientific, 1990); Translated from Russian: *Mekhanicheskoe Deistvie Sveta na Atomy* (Moscow: Nauka, 1991)
- Raab E L et al. *Phys. Rev. Lett.* **59** 2631 (1987)
- Lett P D et al. *Phys. Rev. Lett.* **61** 169 (1988)
- Dalibard J, Cohen-Tannoudji C J. *Opt. Soc. Am. B* **6** 2023 (1989)
- Aspect A et al. *J. Opt. Soc. Am. B* **6** 2112 (1989)
- Anderson M H et al. *Science* **269** 198 (1995)
- Bradley C C et al. *Phys. Rev. Lett.* **75** 1687 (1995)
- Davis K B et al. *Phys. Rev. Lett.* **75** 3969 (1995)
- Pitaevskii L P *Phys. Usp.* **41** 569 (1998); *Usp. Fiz. Nauk* **168** 641 (1998)
- Chu S *Rev. Mod. Phys.* **70** 685 (1998); *Usp. Fiz. Nauk* **169** 274 (1999)
- Cohen-Tannoudji C N *Rev. Mod. Phys.* **70** 707 (1998); *Usp. Fiz. Nauk* **169** 292 (1999)
- Phillips W D *Rev. Mod. Phys.* **70** 721 (1998); *Usp. Fiz. Nauk* **169** 305 (1999)
- Cornell E A, Wieman C E *Rev. Mod. Phys.* **74** 875 (2002); *Usp. Fiz. Nauk* **173** 1320 (2003)
- Ketterle W *Rev. Mod. Phys.* **74** 1131 (2002); *Usp. Fiz. Nauk* **173** 1339 (2003)
- Pitaevskii L P *Phys. Usp.* **49** 333 (2006); *Usp. Fiz. Nauk* **176** 345 (2006)
- Kolachevsky N N *Phys. Usp.* **51** 1180 (2008); *Usp. Fiz. Nauk* **178** 1225 (2008)
- Kolachevsky N N, Khabarova K Yu *Phys. Usp.* **57** 1230 (2014); *Usp. Fiz. Nauk* **184** 1354 (2014)
- Balykin V I *Phys. Usp.* **54** 844 (2011); *Usp. Fiz. Nauk* **181** 875 (2011)
- Wineland D J *Rev. Mod. Phys.* **85** 1103 (2013); *Usp. Fiz. Nauk* **184** 1089 (2014)
- Metcalf H J, van der Straten P *Laser Cooling and Trapping* (New York: Springer, 1999)
- Allan D W *Proc. IEEE* **54** 221 (1966)
- Riehle F *Frequency Standards: Basics and Applications* (Weinheim: Wiley-VCH, 2004); Translated into Russian: *Standarty Chastoty. Printsipy i Prilozheniya* (Moscow: Fizmatlit, 2009)
- Paul W *Rev. Mod. Phys.* **62** 531 (1990); *Usp. Fiz. Nauk* **160** (12) 109 (1990)
- Wineland D J, Dehmelt H G *Bull. Am. Phys. Soc.* **20** 637 (1975)
- Bollinger J J et al. *Phys. Rev. Lett.* **54** 1000 (1985)
- Berkeland D J et al. *Phys. Rev. Lett.* **80** 2089 (1998)
- Oskay W H et al. *Phys. Rev. Lett.* **97** 020801 (2006)
- Rosenband T et al. *Phys. Rev. Lett.* **98** 220801 (2007)
- Fortier T M et al. *Phys. Rev. Lett.* **98** 070801 (2007)
- Peik E, Schneider T, Tamm Chr J. *Phys. B At. Mol. Opt. Phys.* **39** 145 (2006)
- Rosenband T et al. *Science* **319** 1808 (2008)
- Katori H, in *Proc. of the 6th Symp. on Frequency Standards and Metrology* (Ed. P Gill) (Singapore: World Scientific, 2002) p. 323
- Katori H et al. *Phys. Rev. Lett.* **91** 173005 (2003)
- Takamoto M, Katori H *Phys. Rev. Lett.* **91** 223001 (2003)
- Chou C W et al. *Phys. Rev. Lett.* **104** 070802 (2010)
- Madej A A et al. *Phys. Rev. Lett.* **109** 203002 (2012)
- Dubé P et al. *Phys. Rev. Lett.* **112** 173002 (2014)
- Huntemann N et al., in *Program and Book of Abstracts of 8-th Symp. on the Frequency Standards and Metrology, Potsdam, Germany, 12–16 October 2015* (Ed. F Riehle) (Potsdam: Physikalisch-Technische Bundesanstalt, 2015) p. 38
- Takamoto M et al. *Nature* **435** 321 (2005)
- Ludlow A D et al. *Phys. Rev. Lett.* **96** 033003 (2006)
- Brusch A et al. *Phys. Rev. Lett.* **96** 103003 (2006)
- Barber Z W et al. *Phys. Rev. Lett.* **96** 083002 (2006)
- Ludlow A D et al. *Science* **319** 1805 (2008)
- Poli N et al. *Phys. Rev. A* **77** 050501(R) (2008)
- Nicholson T L et al. *Phys. Rev. Lett.* **109** 230801 (2012)
- Hinkley N et al. *Science* **341** 1215 (2013)
- Bloom B J et al. *Nature* **506** 71 (2014)
- Beloy K et al. *Phys. Rev. Lett.* **113** 260801 (2014)
- Ushijima I et al. *Nature Photon.* **9** 185 (2015)
- Nicholson T L et al. *Nature Commun.* **6** 6896 (2015)

63. Riehle F *Physics* **5** 126 (2012)
64. Wynands R, Weyers S *Metrologia* **42** S64 (2005)
65. Jefferts S R et al. *Phys. Rev. Lett.* **112** 050801 (2014)
66. Bagayev S N et al., in *Proc. of the 10-th Intern. Conf. on Laser Spectroscopy* (Eds M Ducloy, E Giacobino, G Camy) (Singapore: World Scientific, 1992) p. 91
67. Hall J L *Rev. Mod. Phys.* **78** 1279 (2006); *Usp. Fiz. Nauk* **176** 1353 (2006)
68. Hänsch T W *Rev. Mod. Phys.* **78** 1297 (2006); *Usp. Fiz. Nauk* **176** 1368 (2006)
69. Baklanov Y V, Chebotaev V P *Appl. Phys.* **12** 97 (1977)
70. Eckstein J N, Ferguson A I, Hänsch T W *Phys. Rev. Lett.* **40** 847 (1978)
71. Ludlow A D et al. *Rev. Mod. Phys.* **87** 637 (2015)
72. Santra R et al. *Phys. Rev. Lett.* **94** 173002 (2005)
73. Zanon-Willette T et al. *Phys. Rev. Lett.* **97** 233001 (2006)
74. Hong T et al. *Phys. Rev. Lett.* **94** 050801 (2005)
75. Taichenachev A V et al. *Phys. Rev. Lett.* **96** 083001 (2006)
76. Varshalovich D A, Moskalev A N, Khersonskii V K *Quantum Theory of Angular Momentum* (Singapore: World Scientific, 1988); Translated from Russian: *Kvantovaya Teoriya Uglovogo Momenta* (Moscow: Nauka, 1975)
77. Baillard X et al. *Opt. Lett.* **32** 1812 (2007)
78. Derevianko A, Katori H *Rev. Mod. Phys.* **83** 331 (2011)
79. Hobson R et al. *Phys. Rev. A* **93** 010501(R) (2016); arxiv:1510.08144
80. Kulosa A P et al. *Phys. Rev. Lett.* **115** 240801 (2015); arxiv:1508.01118
81. Yudin V I et al. *Phys. Rev. A* **82** 011804(R) (2010)
82. Huntemann N et al. *Phys. Rev. Lett.* **109** 213002 (2012)
83. Tabatchikova K S et al. *JETP* **120** 203 (2015); *Zh. Eksp. Teor. Fiz.* **147** 233 (2015)
84. Zanon-Willette T, Yudin V I, Taichenachev A V *Phys. Rev. A* **92** 023416 (2015)
85. Becker Th et al. *Phys. Rev. A* **63** 051802(R) (2001)
86. Schneider T, Peik E, Tamm Chr *Phys. Rev. Lett.* **94** 230801 (2005)
87. Akatsuka T, Takamoto M, Katori H *Nature Phys.* **4** 954 (2008)
88. Lemke N D et al. *Phys. Rev. Lett.* **103** 063001 (2009)
89. Porsev S G, Derevianko A *Phys. Rev. A* **74** 020502(R) (2006)
90. Heavner T P *IEEE Trans. Instrum. Meas.* **54** 842 (2005)
91. Yudin V I et al. *Phys. Rev. Lett.* **107** 030801 (2011)
92. Tamm Chr et al. *Phys. Rev. A* **80** 043403 (2009)
93. Hosaka K et al. *Phys. Rev. A* **79** 033403 (2009)
94. Sherstov I et al. *Phys. Rev. A* **81** 021805(R) (2010)
95. Lea S N, Webster S A, Barwood G P, in *Proc. of the 20th European Frequency and Time Forum, 27–30 March 2006, Braunschweig, Germany* (Ed. F Riehle) (Braunschweig: Physikalisch-Technische Bundesanstalt, 2006) p. 302